ARCHIVES OF MECHANICS
Arch. Mech. **73** (1), 3–26, 2021, DOI: 10.24423/aom.3597

Magnetothermoelastic vibrations on a viscoelastic microbeam subjected to a laser heat source

A. E. ABOUELREGAL[1,3], A. M. ZENKOUR[2]

[1] *Department of Mathematics, College of Science and Arts, Jouf University, Al-Qurayyat, Saudi Arabia*

[2] *Department of Mathematics, Faculty of Science, Kafrelsheikh University, Kafrelsheikh 33516, Egypt, e-mail: zenkour@sci.kfs.edu.eg*

[3] *Department of Mathematics, Faculty of Science, Mansoura University, Mansoura 35516, Egypt*

The linear theory of viscoelasticity remains an important field of research like most solids and polymer materials when exposed to a vicious dynamic loading effect. This article introduces a new model for describing the behavior of thermo-viscoelastic microbeams considering the effects of temperature change and the longitudinal magnetic field. The governing equations in this model are derived based on the Euler–Bernoulli beam theory, Kelvin–Voigt model of viscosity, the generalized thermoelasticity, and the classical Maxwell equations. The two ends of the microbeam are clamped and subjected to the influence of a laser pulse with a temporal intensity profile. The analytical solutions to the physical fields are evaluated using the Laplace transform and its inversion transforms are performed numerically. The thermo-viscoelastic responses of the microbeam are calculated numerically and investigated graphically. The effect of different parameters such as viscosity, laser intensity, and the magnitude of the magnetic field are studied in detail.

Key words: thermoviscoelasticity, microbeams, laser pulse, magnetic field.

Notation

λ, μ	Lame's constants,
α_t	thermal expansion coefficient,
$\gamma = E\alpha_t/(1-2\nu)$	coupling parameter,
T_0	environmental temperature,
$\theta = T - T_0$	temperature increment,
T	absolute temperature,
C_E	specific heat,
e	cubical dilatation,
σ_{ij}	nonlocal stress tensor,
e_{ij}	strain tensor,
L	microbeam length,

$A = bh$	cross-section area,
α_1, α_2	viscoelastic relaxation times,
μ_0	magnetic permeability,
τ_q	phase-lag of heat flux,
ν	Poisson's ratio,
M_T	thermal moment,
q_i	components of the heat flows vector,
K	thermal conductivity,
w	lateral deflection,
q_i	components of heat flows vector,
δ_{ij}	Kronecker's delta tensor,
u	axial displacement,
F_i	body force components,
Q	heat source,
t_0	pulse width,
h	nanobeam thickness,
ρ	material density,
b	microbeam width,
$oxyz$	Cartesian coordinate,
∇^2	Laplacian operator,
E	Young's modulus,
τ_θ	phase-lag of temperature gradient,
$I = bh^3/12$	inertia moment,
IE	flexural rigidity.

1. Introduction

Laser pulse technology has wide applications in material processing, characterization, and non-destructive detection. Also, laser, ultrasound is an innovation where a laser is used to produce and test, ultrasound and includes acoustics, optics, calorific, material, electrics, physic, and so on. Laser ultrasound has many fascinating and interesting points. For example, it is non-contact, fast, non-destructive, and accurate and requires a small effort [1-4]. When the laser affects the microbeams, a portion of the photons is absorbed by the microbeam and their energy is turned to heat while the other photons are reflected. Absorbed heat energy leads to non-uniform thermal stresses, resulting in the vibration of the microbeams [5].

The thermal vibration of bars has led to earth importance in space spacecraft, turbines, reactor vessels, and other machine parts that are exposed to varying heating. Very fast thermal procedures, under the action of a laser heartbeat, are fascinating from the point of view of thermoelasticity, because it requires the investigation of the coupled strain and temperature fields. This indicates the absorption of the energy results of the laser strikes at a limited expansion temperature, causing thermal expansion and creating rapid movements in the structure components, thus bringing a rise of vibrations. Because the duration

of the laser pulse is very short, there will be a very rapid heating process and Fourier's law of heat conduction won't be valid anymore as well as non-Fourier equation of heat conduction that takes into consideration the limited speed of thermal signal propagation [6–8].

Isotropic and anisotropic materials are now commonly used in various engineering fields, including mechanical engineering, aerospace, chemistry, and energy. These materials help to make a device with optimal output in many constructions, such as flats, beams, shells, and curved structures. In a broad variety of applications Microelectromechanical devices (MEMS), Nanoelectromechanical systems (NEMS), and Atomic Force Microscopes, such as an actuator, microswitch, micro-resonator, and AFMS, are increasingly being considered, in which the thicknesses and lengths of microbeams are usually in the order of microns and sub microns [9–15].

Over recent years the main structures commonly used in microsensors, microsoners, microscopes, micro-switches, microfluidic systems have been MEMS-based microbeams. A significant number of researches is therefore carried out to predict and understand the static and dynamic conduct of microbeams [16–20]. Microbeams are also increasingly being considered for different applications. A lot of investigators have discussed the vibration and thermal process of the microbeams [21–27]. Usually, micro/nanobeam or micro/nanoplates are also modeled on MEMS/NEMS. When studying these structures, the classical elastic theory is no longer successful. Several theories have also been established for higher-order continuum theory, such as the theory of non-local elasticity [28], surface elasticity [29], strain gradient [30], micropolar theory [31], and couple stress theory [32, 33].

Studying the viscous behavior of viscous materials such as in bone and bioprotective materials is of interest in various contexts. The linear theory of viscoelasticity is still a significant area of research as most solids and polymer materials when exposed to a dynamic loading manifest a viscous effect. Viscoelasticity is of interest in solid-state physics, materials science, and metallurgy because it is causally linked to a variation of microphysical processes and can be used as an experimental investigation of those procedures. Hooke's law can be approximated for different materials by the linear theory of viscoelasticity. Many investigators have dealt with several thermo-viscoelastic problems by using the generalized models of thermoelasticity [34–41].

The combination of temperature and deformation is an important factor that is commonly disregarded in the literature on microbeams. In simplifying estimates, the viscosity between nanoscale microbeams is also often neglected. This paper analyzes for the first time the viscosity of dynamics microbeams using, the dual-phase-lag heat conduction equation, Kelvin–Voigt viscosity type, and beam theory of Euler–Bernoulli.

In this work, the vibration analysis of thermos-viscoelastic microbeam under the effects of temperature change and an axial magnetic field is investigated. The equations of motion and heat conduction are derived by using the generalized thermoelastic model with phase lags. This paper also, which produces linear coupling used the Kelvin–Voigt viscosity model. The influences of the magnetic field and laser intensity of the vibration behavior of the microbeam is investigated and discussed in detail. Moreover, numerical results are illustrated to investigate the effect of parameters of viscoelastic medium and phase lags.

2. Mathematical modeling

The structure under investigation is a Kelvin–Voigt type thermo-viscoelastic microbeam of length L, thickness h, and width b (Fig. 1). The microbeam is heated uniformly by a laser pulse, fully submerged in a longitudinal magnetic field, and subjected to varying sinusoidal pulse temperature. It is assumed that the microbeam is thin enough so that the Euler–Bernoulli beam theory is sufficient to describe the mechanical behavior of the microbeam. The x-coordinate is parallel to the axis of the microbeam while the thickness and width directions are parallel to the y- and z-axes, respectively. Also, the microbeam can be demonstrated as a prism microbeam with either simply supported or doubly clamped ends.

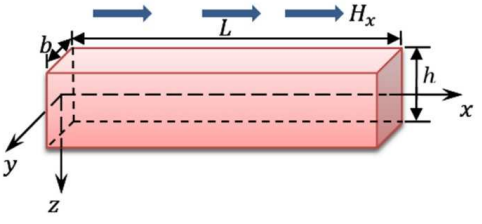

Fig. 1. Schematic of the microbeam under the longitudinal magnetic field.

The displacements are given as

$$u = -z\frac{\partial w}{\partial x}, \qquad v = 0, \qquad w = w(x, z, t). \tag{2.1}$$

The thermoelastic stress field in the slender microbeam is supposed to be uniaxial; only the axial stress σ_{xx} can attained non-zero values [42].

The use of viscoelastic models is important, instead of an elastic model, to effectively model the dynamic behavior of microbeams. Viscosity can be integrated into the dynamic model of the popular Maxwell, Kelvin–Voigt, linear standard,

in solid mechanically. In this paper, the Kelvin–Voigt viscosity model produces linear couples. According to the Kelvin–Voigt scheme, the axial stress σ_{xx} of the viscoelastic microscale microbeam can be expressed as [43]:

$$\sigma_{xx} = (2\mu^* + \lambda^*)\frac{\partial u}{\partial x} - \beta^*\theta, \tag{2.2}$$

The viscoelastic parameters μ^*, λ^* and β^* are expressed as [44, 45]

$$\begin{aligned} &\lambda^* = \lambda\left(1 + \alpha_1\frac{\partial}{\partial t}\right), \quad \mu^* = \mu\left(1 + \alpha_2\frac{\partial}{\partial t}\right), \quad \beta^* = \beta_0\left(1 + \beta_v\frac{\partial}{\partial t}\right), \\ &\beta_0 = (3\lambda + 2\mu)\alpha_t, \quad \beta_v = \frac{(3\lambda\alpha_1 + 2\mu\alpha_2)\alpha_t}{\beta_0}. \end{aligned} \tag{2.3}$$

The flexure moment of the beams $M(x,t)$ is given by:

$$M(x,t) = -b\int\limits_{-h/2}^{h/2} z\sigma_{xx}\,\mathrm{d}z. \tag{2.4}$$

Substituting Eq. (2.2) into Eq. (2.4), one has

$$M(x,t) = I(2\mu^* + \lambda^*)z\frac{\partial^2 w}{\partial x^2} + \beta^* M_T \tag{2.5}$$

where

$$M_T = b\int\limits_{-h/2}^{h/2} z\theta(x,z,t)\,\mathrm{d}z. \tag{2.6}$$

After applying the initial magnetic field $\vec{H}$ and current density $\vec{J}$, one gets as a result of an induced magnetic field $\vec{h}$ and an induced electric field $\vec{E}$. Maxwell's electromagnetic field equations for a homogeneous and electrically perfect conducting medium may be defined as [46]

$$\begin{aligned} &\vec{J} = \nabla\times\vec{h}, \quad \nabla\times\vec{E} = -\mu_0\frac{\partial\vec{h}}{\partial t}, \quad \vec{E} = -\mu_0(\frac{\partial\vec{u}}{\partial t}\times\vec{H}), \\ &\vec{h} = \nabla\times(\vec{u}\times\vec{H}), \quad \nabla\cdot\vec{h} = 0. \end{aligned} \tag{2.7}$$

The application of the longitudinal magnetic field $\vec{H} \equiv (H_x, 0, 0)$ in the axial direction of the microbeam. We can write the vector of the induced magnetic field $\vec{h}$ and current density $\vec{J}$ after using Eq. (2.1) in the following forms:

$$\vec{h} = \nabla \times (\vec{u} \times \vec{H}) = \nabla \times \begin{vmatrix} e_x & e_y & e_z \\ u & 0 & w \\ H_x & 0 & 0 \end{vmatrix} \equiv H_x \left(0, 0, \frac{\partial w}{\partial x}\right),$$

$$\vec{J} = \nabla \times \vec{h} = H_x \begin{vmatrix} e_x & e_y & e_z \\ \frac{\partial}{\partial x} & \frac{\partial}{\partial y} & \frac{\partial}{\partial z} \\ 0 & 0 & \frac{\partial w}{\partial x} \end{vmatrix} \equiv -H_x \left(0, \frac{\partial^2 w}{\partial x^2}, 0\right). \tag{2.8}$$

Using the previous equation, Eq. (2.8), into Lorentz force $\vec{F}$ that induced by applying the longitudinal magnetic field $\vec{H}$, yields [47]

(2.9)

$$\vec{F} \equiv (f_x, f_y, f_z) \equiv \mu_0(\vec{J} \times \vec{H}) = -\mu_0 H_x \begin{vmatrix} e_x & e_y & e_z \\ 0 & \frac{\partial^2 w}{\partial x^2} & 0 \\ H_x & 0 & 0 \end{vmatrix} \equiv \mu_0 H_x^2 \left(0, 0, \frac{\partial^2 w}{\partial x^2}\right).$$

For transverse vibration of microbeams, the equilibrium equation can be written as [47]

$$\frac{\partial^2 M}{\partial x^2} + \rho A \frac{\partial^2 w}{\partial t^2} + f(x) = 0 \tag{2.10}$$

where $f(x)$ is a function of space that incorporates the longitudinal magnetic force. Here $f(x) \neq f_z$, since f_z denotes a body force and $f(x)$ represents the force per length. So, $f(x)$ is expressed as

$$f(x) = A f_z = A\mu_0 H_x^2 \frac{\partial^2 w}{\partial x^2}. \tag{2.11}$$

Let us consider that there is no heat flow across the surfaces of the microbeam, so that $\frac{\partial \theta}{\partial x} = 0$ at $z = \pm\frac{h}{2}$. According to this assumption, we take the variation of temperature increment as

$$\theta(x, z, t) = \phi(x, t) \sin(pz), \qquad p = \frac{\pi}{h}. \tag{2.12}$$

Introducing Eqs. (2.12) into Eq. (2.6), one has

$$M_T = 2ap^2 \phi(x, t). \tag{2.13}$$

The substitution of Eq. (2.13) into Eq. (2.5), and Eq. (2.5) into Eq. (2.10), gives

$$M(x, t) = I(2\mu^* + \lambda^*) z \frac{\partial^2 w}{\partial x^2} + 2ap^2 \beta^* \phi(x, t), \tag{2.14}$$

$$I(2\mu^* + \lambda^*) \frac{\partial^4 w}{\partial x^4} + \rho A \frac{\partial^2 w}{\partial t^2} + 2ap^2 \beta^* \frac{\partial^2 \phi}{\partial x^2} + A\mu_0 H_x^2 \frac{\partial^2 w}{\partial x^2} = 0. \tag{2.15}$$

The classical theory of coupled thermoelasticity meant an infinite rate of propagation of thermal signals and this counteracts physical facts. During the last four decades, generalized theories including finite speed of heat transportation in thermoelastic mediums have been advanced to eliminate this absurdity. The relevant theoretical developments on the subject are due to Tzou [48, 49] called dual-phase-lag model (DPL) for heat transport mechanism. In this model, Tzou presented two phase-lags to both the temperature gradient τ_θ and the heat flux vector τ_q. The generalized model of heat conduction equation with phase-lags is given by [50]:

$$K\left(1+\tau_\theta\frac{\partial}{\partial t}\right)\theta_{,ii}=\left(\delta+\tau_q\frac{\partial}{\partial t}\right)\left[\rho C_E\frac{\partial\theta}{\partial t}+\beta^* T_0\frac{\partial e}{\partial t}-\rho Q\right]. \tag{2.16}$$

The model in Eq. (2.16) is said to be a hyperbolic heat conduction model since it contains the second-order derivative of temperature versus time. If $\tau_q > \tau_\theta$, the local heat flux vector is the result of the temperature gradient in the same place but early. That is, if $\tau_q < \tau_\theta$ the temperature gradient is the result of the heat flux early. For more details on Eq. (2.16), one can refer to [51–56].

In absence of PL for temperature gradient ($\tau_\theta = 0$), Eq. (2.16) is simplified to the hyperbolic conduction model proposed by Lord and Shulman (LS) [57]. Under the Euler–Bernoulli assumption, the heat conduction equation (2.16), becomes

$$K\left(1+\tau_\theta\frac{\partial}{\partial t}\right)\left(\frac{\partial^2}{\partial x^2}+\frac{\partial^2}{\partial z^2}\right)\theta=\left(1+\tau_q\frac{\partial}{\partial t}\right)\left[\rho C_E\frac{\partial\theta}{\partial t}-\beta^* T_0 z\frac{\partial^3 w}{\partial x^2\partial t}-\rho Q\right]. \tag{2.17}$$

For $\tau_q = \tau_\theta = 0$, this is identical with classical heat conduction Fourier's law. In addition, in the absence of viscous effect the viscoelastic relaxation times should have vanished (i.e., $\alpha_1 = \alpha_2 = 0$).

The laser heat source term with an ultra-short pulse duration t_p and intensity L_0 is given as follows [58, 59]:

$$Q(z,t)=\frac{R_a}{\delta_0}\bar{I}(t)\mathrm{e}^{\frac{2z-h}{2\delta_0}}=\frac{L_0 R_a}{\delta_0 t_p^2}t\mathrm{e}^{(\frac{2z-h}{2\delta_0}-\frac{t}{t_p})} \tag{2.18}$$

where R_a is surface reflectivity, δ_0 is optical penetration depth and $\bar{I}$(t) is the non-Gaussian temporal profile which is given by [59]:

$$\bar{I}(t)=\frac{L_0}{t_p^2}t\mathrm{e}^{-\frac{t}{t_p}}. \tag{2.19}$$

It is obvious that the maximum laser intensity is decreasing with the increase in t_p. According to [59], the conduction in the microbeam is displayed as a 1D problem with a heat source $Q(z,t)$ given by:

$$Q(z,t) = \frac{R_a}{\delta_0}\bar{I}(t)\mathrm{e}^{\frac{2z-h}{2\delta_0}} = \frac{L_0 R_a}{\delta_0 t_p^2} t\mathrm{e}^{(\frac{2z-h}{2\delta_0}-\frac{t}{t_p})} \tag{2.20}$$

where δ_0 denotes the absorptive depth of heating energy and R_a represents absorptivity of the irradiated surface. Using Eqs. (2.12), (2.19), the heat equation (2.17) can be written as

$$\begin{aligned}\sin(pz)\left(1+\tau_\theta\frac{\partial}{\partial t}\right)\left(\frac{\partial^2}{\partial x^2}-p^2\right)\phi \\ = \left(\delta+\tau_q\frac{\partial}{\partial t}\right)\left[\frac{\rho C_E}{K}\sin(pz)\frac{\partial\phi}{\partial t}-\frac{\beta^* T_0}{K}z\frac{\partial^3 w}{\partial x^2\partial t}-\frac{\rho I_0 R_a}{K\delta_0 t_p^2}t\mathrm{e}^{(\frac{2z-h}{2\delta_0}-\frac{t}{t_p})}\right].\end{aligned} \tag{2.21}$$

Multiplying the previous equation by z and integrating zfrom $-h/2$ to $h/2$ with respect to z, we obtain

$$\left(1+\tau_\theta\frac{\partial}{\partial t}\right)\left(\frac{\partial^2}{\partial x^2}-p^2\right)\phi = \left(\delta+\tau_q\frac{\partial}{\partial t}\right)\left[\eta_0\frac{\partial\phi}{\partial t}-\beta^*\eta_1\frac{\partial^3 w}{\partial x^2\partial t}-\eta_2 f(t)\right] \tag{2.22}$$

where

$$\begin{aligned}&\eta_0 = \frac{\rho C_E}{K}, \quad \eta_1 = \frac{T_0 h^3}{2p^2 K}, \\ &\eta_2 = \frac{\rho L_0 R_a \delta_0}{2p^2 K t_p^2}\left[\frac{h}{2\delta_0}-1+\left(\frac{h}{2\delta_0}+1\right)\mathrm{e}^{\frac{-h}{\delta_0}}\right], \quad f(t) = t\mathrm{e}^{-\frac{t}{t_p}}.\end{aligned} \tag{2.23}$$

3. Dimensionless quantities

In terms of the non-dimensional quantities

$$\begin{aligned}&\{x', w', u', z', L', b'\} = c_1\eta_0\{x, w, u, z, L, b\}, \quad \{t', \tau_q', \tau_\theta'\} = c_1^2\eta_0\{t, \tau_q, \tau_\theta\}, \\ &\theta' = \frac{\beta}{\rho c_1^2}\theta, \quad \sigma_{xx}' = \frac{1}{\rho c_1^2}\sigma_{xx}, \quad Q' = \frac{1}{K c_1^2\eta_2^2 T_0}Q, \quad c_1^2 = \frac{2\mu+\lambda}{\rho},\end{aligned} \tag{3.1}$$

the governing equations (2.15), (2.22), and (2.2) can be written as

$$\left(1+c_2^2\frac{\partial}{\partial t}\right)\frac{\partial^4 w}{\partial x^4}+\eta_3\frac{\partial^2 w}{\partial t^2}+\eta_4\left(1+\beta_1\frac{\partial}{\partial t}\right)\frac{\partial^2\phi}{\partial x^2}+a_0^2\eta_3\frac{\partial^2 w}{\partial x^2} = 0, \tag{3.2}$$

$$\begin{aligned}\left(1+\tau_\theta\frac{\partial}{\partial t}\right)\left(\frac{\partial^2}{\partial x^2}-p^2\right)\phi \\ = \left(\delta+\tau_q\frac{\partial}{\partial t}\right)\left[\frac{\partial\phi}{\partial t}-\varepsilon\eta_5\left(1+\beta_1\frac{\partial}{\partial t}\right)\frac{\partial^3 w}{\partial x^2\partial t}-\eta_6 f(t)\right],\end{aligned} \tag{3.3}$$

$$\sigma_{xx} = -z\left(1+\eta_0 c_2^2\frac{\partial}{\partial t}\right)\frac{\partial^2 w}{\partial x^2}-\sin(pz)\left(1+\beta_1\frac{\partial}{\partial t}\right)\phi \tag{3.4}$$

where

$$c_2^2=\frac{\alpha_1\lambda+2\mu\alpha_2}{\rho},\quad \eta_3=\frac{12}{h^2},\quad \eta_4=\frac{24p^2c_1^5\eta_0}{h^3},\quad \eta_5=\frac{h^3}{2p^2c_1^6\eta_0^4},$$
$$a_0^2=\frac{\mu_0H_x^2}{\rho},\quad \eta_6=\frac{\beta\eta_2}{\rho c_1^4\eta_0^3},\quad \varepsilon=\frac{\beta^2T_0}{\rho^2C_Ec_1^2}. \tag{3.2}$$

4. Solution of the problem

The considered field variables can be obtained by using the mechanism of the Laplace transform. So, the following initial conditions should be considered

$$w(x,t)|_{t=0}=\left.\frac{\partial w(x,t)}{\partial t}\right|_{t=0}=0,\qquad \phi(x,t)|_{t=0}=\left.\frac{\partial\phi(x,t)}{\partial t}\right|_{t=0}=0. \tag{4.1}$$

After using Laplace transform the field equations Eqs. (3.2)–(3.4) can be given by

$$\frac{\mathrm{d}^4\bar{w}}{\mathrm{d}x^4}+A_0\frac{\mathrm{d}^2\bar{w}}{\mathrm{d}x^2}+A_1\bar{w}+A_2\frac{\mathrm{d}^2\bar{\phi}}{\mathrm{d}x^2}=0, \tag{4.2}$$

$$\left(\frac{\mathrm{d}^2}{\mathrm{d}x^2}-A_3\right)\bar{\phi}=-A_4\frac{\mathrm{d}^2\bar{w}}{\mathrm{d}x^2}-A_5\bar{g}(s), \tag{4.3}$$

$$\bar{\sigma}_{xx}=-(1+\eta_0c_2^2s)z\frac{\mathrm{d}^2\bar{w}}{\mathrm{d}x^2}-\sin(pz)(1+\beta_1s)\bar{\phi} \tag{4.4}$$

where

$$A_1=\frac{s^2\eta_3}{1+sc_2^2},\quad A_2=\frac{\eta_4(1+\beta_1s)}{1+sc_2^2},\quad A_0=\frac{a_0^2\eta_3}{1+sc_2^2},$$
$$A_3=p^2+q,\quad q=\frac{s(\delta+\tau_qs)}{1+\tau_\theta s}, \tag{4.5}$$
$$A_4=q\eta_5\varepsilon(1+\beta_1s),\quad A_5=q\eta_6,\quad \bar{g}(s)=\left(\frac{t_p}{1+t_ps}\right)^2.$$

Eliminating $\bar{\phi}(x)$ between Eqs. (4.2) and (4.3), one obtains a differential equation satisfied by $\bar{w}$ as

$$\frac{\mathrm{d}^6\bar{w}}{\mathrm{d}x^6}-a_1\frac{\mathrm{d}^4\bar{w}}{\mathrm{d}x^4}+a_2\frac{\mathrm{d}^2\bar{w}}{\mathrm{d}x^2}-a_3\bar{w}=0, \tag{4.6}$$

where the coefficients a_1, a_2 and a_3 are presented by

$$a_1=A_2A_4+A_3-A_0,\quad a_2=A_1-A_0A_3,\quad a_3=A_1A_3. \tag{4.7}$$

The general solutions of Eqs. (4.6) can be expressed as

$$\bar{w} = \sum_{j=1}^{3} (C_j \mathrm{e}^{-k_j x} + C_{j+3} \mathrm{e}^{k_j x}) \tag{4.8}$$

where k_1^2, k_2^2 and k_3^2 are the roots of

$$k^6 - a_1 k^4 + a_2 k^2 - a_3 = 0. \tag{4.9}$$

These roots are expressed as [58]

$$k_i^2 = \frac{1}{3}[\psi_i (2a_1^3 + 27a_3 - 9a_1 a_2)^{1/3} + a_2], \quad i = 1, 2, 3, \tag{4.10}$$

where

$$\begin{aligned} &\{\psi_1, \psi_2, \psi_3\} = -\frac{1}{2}\{2R_0, -R_0 + \mathrm{i}\sqrt{3}R_1, -R_0 - \mathrm{i}\sqrt{3}R_1\}, \\ &R_0 = \frac{\xi^2 - R_0}{\xi}, \quad R_1 = \frac{\xi^2 + R_2}{\xi}, \quad R_2 = \frac{3a_2 - a_1^2}{(2a_1^3 + 27a_3 - 9a_1 a_2)^{2/3}}, \\ &\xi = \frac{1}{2}(4 + 4\sqrt{4R_2^3 + 1})^{1/3}. \end{aligned} \tag{4.11}$$

Introducing Eq. (4.2) in Eq. (4.3), we get

$$\bar{\phi} = \frac{-1}{A_2 A_3}\left(\frac{\mathrm{d}^4 \bar{w}}{\mathrm{d}x^4} + (A_0 - A_2 A_4)\frac{\mathrm{d}^2 \bar{w}}{\mathrm{d}x^2} + A_1 \bar{w} - A_2 A_5 \bar{g}(s)\right). \tag{4.12}$$

Substituting the value of $\bar{w}$ into (4.12), we can express the general solution of temperature $\bar{\theta}$ as

$$\bar{\theta} = \sin(pz) \sum_{j=1}^{3} H_j (C_j \mathrm{e}^{-k_j x} + C_{j+3} \mathrm{e}^{k_j x}) + \sin(pz) H_4 \tag{4.13}$$

where

$$H_j = \frac{-1}{A_2 A_3}(k_j^4 + (A_0 - A_2 A_4)k_j^2 + A_1), \qquad H_4 = \frac{A_5 \bar{g}(s)}{A_3}. \tag{4.14}$$

The displacement $\bar{u}$ after using Eq. (4.8) takes the form

$$\bar{u} = -z\frac{\mathrm{d}\bar{w}}{\mathrm{d}x} = z \sum_{j=1}^{3} k_j (C_j \mathrm{e}^{-k_j x} - C_{j+3} \mathrm{e}^{k_j x}). \tag{4.15}$$

Also, the strain is

$$\bar{e} = -z\frac{d^2\bar{w}}{dx^2} = -z\sum_{j=1}^{3} k_j^2(C_j \mathrm{e}^{-k_j x} + C_{j+3}\mathrm{e}^{k_j x}). \tag{4.16}$$

In addition, the thermal stress $\bar{\sigma}_{xx}$ given in Eq. (4.4) with the aid of Eqs. (4.8) and (4.13), become

$$\bar{\sigma}_{xx} = -\sum_{j=1}^{3}(z(1+\eta_0 c_2^2 s)k_j^2 + \sin(pz)(1+\beta_1 s)H_j)(C_j \mathrm{e}^{-k_j x} + C_{j+3}\mathrm{e}^{k_j x}) - \sin(pz)(1+\beta_1 s)H_4. \tag{4.17}$$

The theories of Lord and Shulman [57] and Green and Naghdi [60] as well as the classical thermoelasticity theory (CTE), are adopted as special cases depending on the values of the PLs τ_q and τ_θ.

5. Applications

The present microbeam is thermally loaded on the boundary $x = 0$ as

$$\theta(0, z, t) = \theta(0, t)\sin(pz) = \theta_0 f(x, t)\sin(pz) \tag{5.1}$$

where θ_0 is a constant. We consider the function $f(x, t)$ is varying with time as a sinusoidal pulse described mathematically as

$$f(x, t) = f(t) = \begin{cases} \sin(\pi/t_0 t), & 0 \le t \le t_0, \\ 0, & t > t_0,\ t < 0, \end{cases} \tag{5.2}$$

where t_0 represents the pulse width of the temperature varying. Furthermore, the temperature at the end boundary satisfies the following relation:

$$\left.\frac{\partial\theta(x, t)}{\partial x}\right|_{x=L} = 0. \tag{5.3}$$

Additionally, since the ends of the microbeam are clamped then,

$$w(x, t)|_{x=0,L} = \left.\frac{\partial w(x, t)}{\partial x}\right|_{x=0,L} = 0. \tag{5.4}$$

In the Laplace transform domain, the boundary conditions in Eqs. (5.1), (5.3) and (5.4) become in the forms

$$\begin{aligned} &\bar{w}(x, s)|_{x=0,L} = \left.\frac{\mathrm{d}\bar{w}(x, s)}{\mathrm{d}x}\right|_{x=0,L} = 0, \\ &\bar{\phi}(x, s)|_{x=0} = \frac{\pi t_0}{\pi^2 + t_0^2 s^2}, \quad \left.\frac{\mathrm{d}\bar{\phi}(x, s)}{\mathrm{d}x}\right|_{x=L} = 0. \end{aligned} \tag{5.5}$$

The replacement of Eqs. (4.8) and (4.13) into Eq. (5.5) yields the unknown parameters C_j, $j = 1, \ldots, 6$.

6. Numerical inversion of Laplace transforms

The solutions for deflection, displacement, temperature, and stress of the present microbeam in the physical field may be obtained by using a numerical inversion technique via a Fourier series expansion. In this procedure, the inverse $g(xt)$ of Laplace transform $\mathrm{g(s)}\bar{g}(\mathrm{x,s})$ is come close to the relation [61]

$$g(x,t) = \frac{\mathrm{e}^{ct}}{t_1}\left[\frac{1}{2}\bar{g}(x,c) + \mathrm{Re}\left\{\sum_{k=1}^{n}\bar{g}\left(x, c + \frac{ik\pi}{t_1}\right)\right\}\right], \quad 0 \le t \le t_1 \tag{6.1}$$

where n denotes a sufficiently large integer. The optimal choice of the free parameter c is obtained according to the criteria described in [61].

7. Discussions of the results

In this section, the thermoelastic dynamic behavior of viscoelastic microscale beams is investigated in detail. The current analysis is validated by comparing calculated outcomes with those available for viscoelastic microbeams. A numerical example is given to study the effect of viscosity, pulse width and the time of laser-pulse as well as the laser intensity parameters on dimensionless lateral vibration w, temperature θ, displacement u and stress σ_{xx} of microbeams along the x-direction. For this purpose, we take the following physical values of copper material

$$\begin{aligned}
&\rho = 8.954 \times 10^3\,\mathrm{kg/m^3}, \quad C_E = 383.1\,\mathrm{J/(kg \cdot K)}, \quad T_0 = 296\,\mathrm{K},\\
&\alpha_t = 1.78 \times 10^{-5}\,\mathrm{K^{-1}}, \quad \lambda = 7.76 \times 10^{10}\,\mathrm{kg/m^3}, \quad \mu = 3.86 \times 10^{10}\,\mathrm{kg/m^3},\\
&K = 386\,\mathrm{W/(m \cdot K)}, \quad E = 8.4 \times 10^{10}\,\mathrm{kg/m^3}, \quad \alpha_1 = 0.6\,\mathrm{s}, \quad \alpha_2 = 0.9\,\mathrm{s},\\
&t = 0.1\,\mathrm{s}, \quad \tau_q = 0.05\,\mathrm{s}, \quad \tau_\theta = 0.01\,\mathrm{s}, \quad \nu = 0.33,\\
&\mu_0 = 1.26 \times 10^{-6}\,\mathrm{Hm^{-1}}, \quad H_x = 10^7\,\mathrm{Am^{-1}}.
\end{aligned}$$

Also, unless otherwise indicated, the value of the parameters R_a, δ_0 and L_0 of the viscoelastic microbeam are taken as 0.5, 0.01 and $10^{11}\,\mathrm{J/m^2}$. Also, we assumed that the ratios of viscoelastic microbeam are fixed as $L/h = 10$ and $b/h = 0.5$. Consequently, when the thickness h is varied, the length L and width b are changed accordingly with h. The results are presented for $L = 1$ and $z = h/6$. The computations are performed for one value of time, namely $t = 0.1$. The intensity of a laser $\bar{L}_0$ ($\bar{L}_0 = 10^{-11}L_0$) is also considered. Various cases of the field variables are studied by clarifying numerical values in Figs. 2–5.

7.1. The effects of viscosity parameters

In this case the variations of the field variables for different values of the viscosity parameters α_1 and α_2 are investigated. The effects of viscosity have been presented in Fig. 2 when the pulse width parameter t_0, time of laser-pulse t_p, laser intensity I_0 and phase-lags τ_q and τ_θ parameters remain constants. It is known that all materials consist of molecules and atoms that are permanently moving. When the temperature is added to a material, the atoms and molecules vibrate faster. As atoms vibrate faster, the space between atoms increases. Movement and particle spacing determine the state of the material from the material then the object expands and takes up more space.

As shown in Fig. 2, we can see that due to the presence of the viscosity term in the phase lag model, the amplitude of the thermoelastic fields has decreased considerably for the viscous microbeam compared with the non-viscous one. Also, it should be noted that all the field quantities vanish identically with the increase

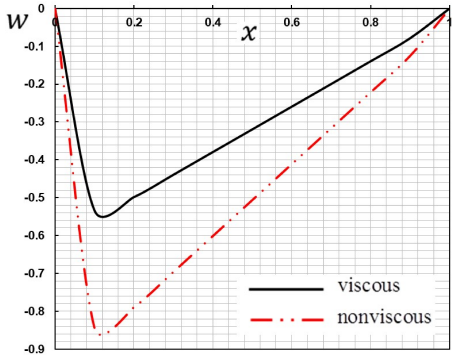

(a) Transverse deflection w versus x.

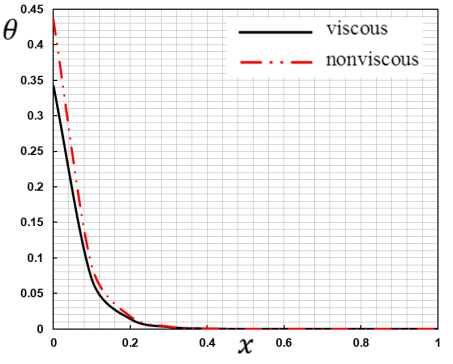

(b) Temperature θ versus x.

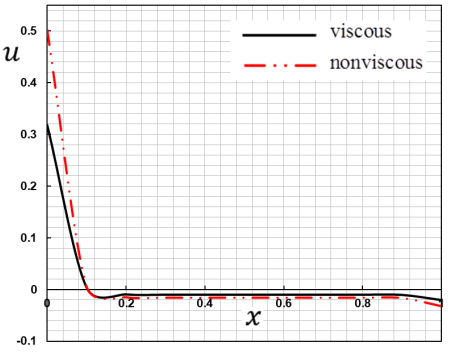

(c) Displacement u versus x.

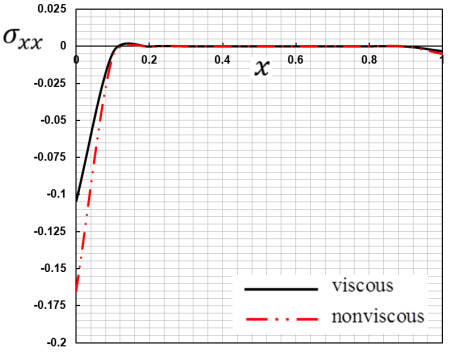

(d) Thermal stress σ_{xx} versus x.

FIG. 2. The transverse deflection, temperature, displacement, and thermal stress distributions of the microbeam for different values of the viscosity parameters α_1 and α_2.

of the length x. Thus, we have found some significant differences in the effect of the two phase-lags τ_θ and τ_q of temperature gradient and heat flux vector on all the physical variables.

Figure 2(a) shows that the lateral vibration distribution w satisfies the boundary condition at the two ends of the microbeam (i.e. vanishes at $x = 0, L$). The microbeam exerts maximum deflection near the first end of the microbeam at all times as compared to that at other points on the axial axis. The deflection w first decreases sharply to its minimum values near $x \cong 0.14$ and then increases slowly to zero values at $x = 1$. The magnitudes of the displacement are decreasing due to the presence of viscosity.

Figure 2(b) illustrates that the behavior of temperature θ starts with maximum values on the boundary of microbeam $x = 0$, thereafter continuously decrease to zero value in the range $0.3 \leq x \leq 1$. As shown in Fig. 2(b), we see that the temperature profile decreases due to viscosity presence.

Figure 2(c) displays the variation of the displacement u behavior versus different values of the viscosity parameters α_1 and α_2. It is observed from Fig. 2(c) that the displacement u starts with a positive value and then decreases continuously to negative values and thereafter continuously increases to zero values for all the two cases. In the axial direction, due to the coupling movement of the device, the excitation thermal load can cause considerable axial displacement.

The effect of the viscosity parameters α_1 and α_2 on the thermal stress σ_{xx}. of the viscoelastic microscale beam is shown in Fig. 2(d). From Fig. 2(d), we can find that the stress σ_{xx} starts with a negative value and then increases continuously to zero values for all the two cases. The presence of viscosity helps to minimize the magnitude of thermal stress.

The velocity of stress diffusion can be observed as being finite and coinciding with the physical behavior of viscoelastic materials. In addition, the boundary is satisfied with these figures. Finally, from the previous conclusions, we can conclude that viscosity has a clear effect on all different distributions. Also, it is of interest that when $\alpha_1 = \alpha_2 = 0$, the results for non-viscoelasticity theory are rendered. Good agreement was observed between the current results and those of Mashat *et al.* [62].

7.2. The effects of the parameter of pulse width t_0 on the field variables

This case is studying how the distributions of deflection, temperature, thermal stress, and displacement vary with the pulse width of the temperature t_0 when the parameters τ_q, τ_θ, t_p, I_0, α_1 and α_2 remain constants. To show the influences of pulse width on all the studied fields of the microbeam, the results for various values of $t_0 = 0.1, 0.15, 0.2$ are highlighted in Fig. 3.

From Fig. 3, it is observed that all the field variables are very sensitive to the variation of the pulse width t_0. Fig. 3(a) reveals that the lateral vibration

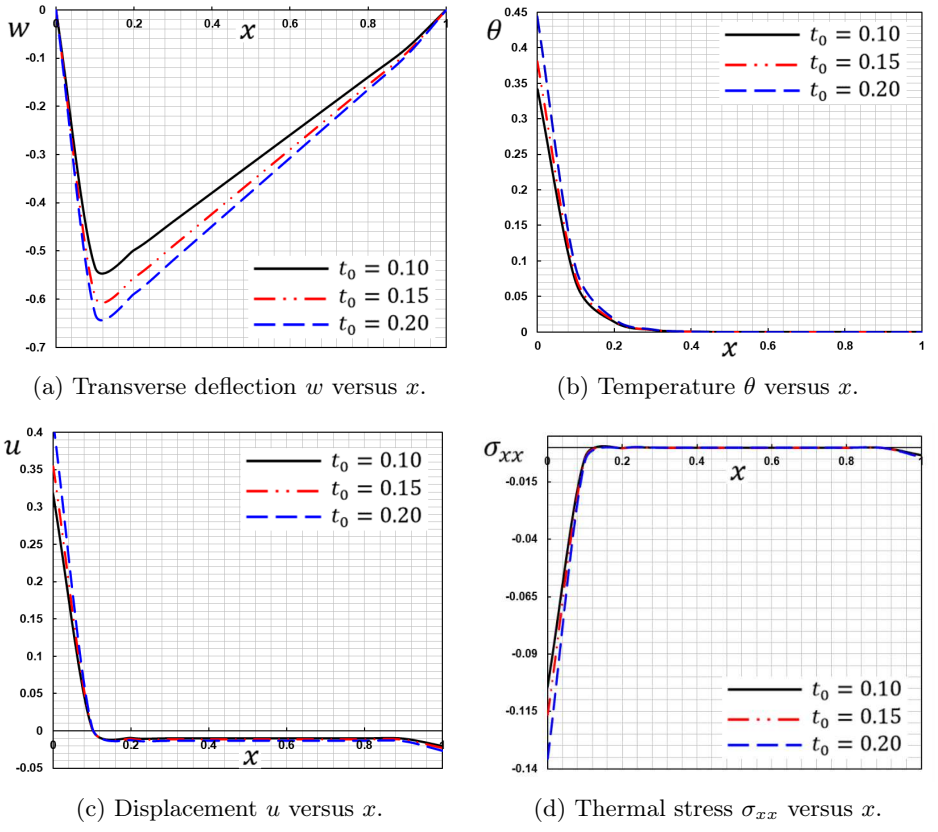

(a) Transverse deflection w versus x.

(b) Temperature θ versus x.

(c) Displacement u versus x.

(d) Thermal stress σ_{xx} versus x.

FIG. 3. The transverse deflection, temperature, displacement, and thermal stress distributions of the microbeam for three different values of the pulse width of the temperature t_0.

w decreases as pulse width increases. The temperature-response curves for the different pulse width parameter t_0 are plotted in Fig. 3(b). It was found that an increase in the values of t_0 increases the temperature values.

The influence of the pulse width parameter t_0 on the response of the displacement u and the thermal stress σ_{xx} of viscoelastic microbeams are shown in Figs. 3(c) and 3(d). From Fig. 3(c), it has been observed that an increased pulse width parameter, significantly increases the displacement behavior. It is worth noting that that thermal stress σ_{xx} of the microbeam is significantly affected by the pulse width parameter of the thermal load.

7.3. The effects of the laser pulse t_p on the field variables

The thermoelastic vibrations due to an axial magnetic field and laser-pulse, the behavior of the field variables with different values of the laser-pulse t_p parameter is investigated. The values of parameters I_0, τ_q, t_0, τ_θ, α_1 and α_2 remain constants.

The laser-pulse effect on the dynamic deflection and temperature of viscoelastic microbeams is illustrated in Fig. 4. Comparing Fig. 4(a–d), it was found that a significant effect of the laser-pulse parameter on all the fields studied was very clear. Figure 4(a) and 4(d) show by increasing the values of the laser-pulse t_p causes an increase in the values of deflection w and thermal stress σ_{xx} which is very evident in the peek points of the curves. As an expected increase in the values of the laser-pulse t_p causes a decrease in the values of temperature (see Fig. 4(b)). As shown in Fig. 4(c), we can see that the displacement values u decrease with the laser parameter in the range $0 \leq x \leq 0.1$, then increase in the range $0.1 \leq x \leq 0.5$.

The so-called ultra-short lasers range from nanoseconds to femtoseconds in general and have pulse length. The high-intensity energy flow and the extremely short laser beam have produced situations in which very wide thermal gradients or an ultra higher heat speed can occur along with the limits of ultra-short laser heating [15–17].

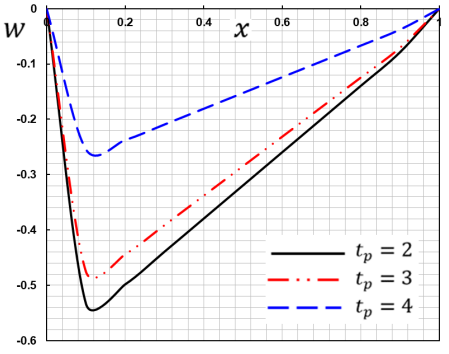

(a) Transverse deflection w versus x.

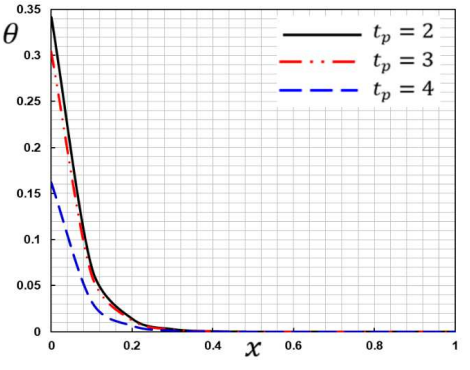

(b) Temperature θ versus x.

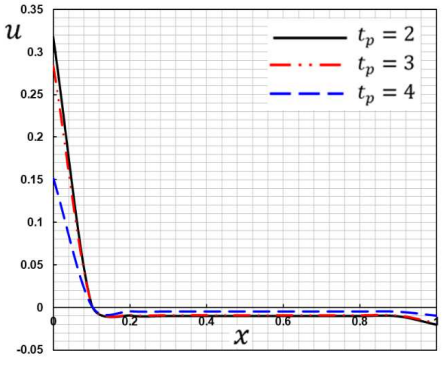

(c) Displacement u versus x.

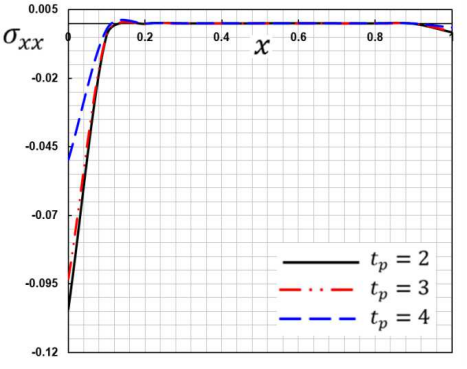

(d) Thermal stress σ_{xx} versus x.

Fig. 4. The transverse deflection, temperature, displacement, and thermal stress distributions of the microbeam for different values of the laser-pulse parameter t_p.

From a physical point of view, when a laser pulse irradiates the top surface of a beam, the heat flow sequentially goes through each infinitesimal part perpendicular to the z-axis. The energy conservation law states that one portion of the heat flux is consumed by the element and increases its intrinsically essential energy, as the temperature increases step by step. Owing to the temperature gradient, the other part of the heat stream tends to disperse through the heat conduction. As the heat fluctuation is continuously absorbed in the spread phase, the amplitude of thermal distortion decreases [17–19].

7.4. The effects of the laser intensity on the field quantities

From Fig. 5, it is clear that when the parameters τ_q, t_0, τ_θ, α_1 and α_2 remain constant, the laser intensity parameter I_0 has an increasing effect on the field variables. As shown in Figs. 5(a) and 5(d), the non-dimensional deflection and stress increase with the increasing of the laser intensity I_0 while temperature and displacement decrease (Figs. 5(b, c)).

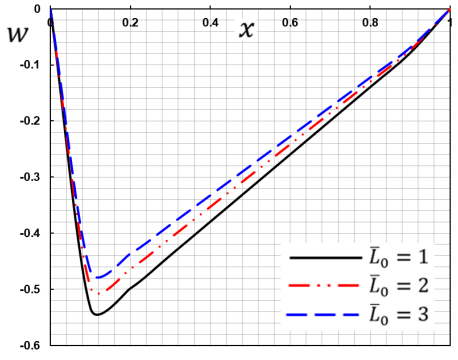

(a) Transverse deflection w versus x.

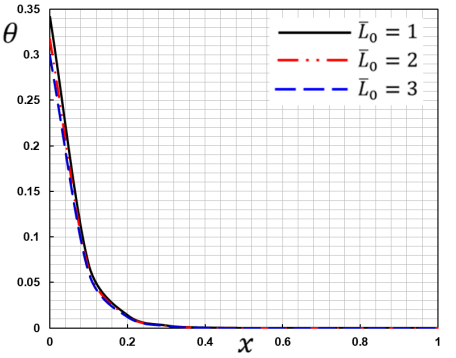

(b) Temperature θ versus x.

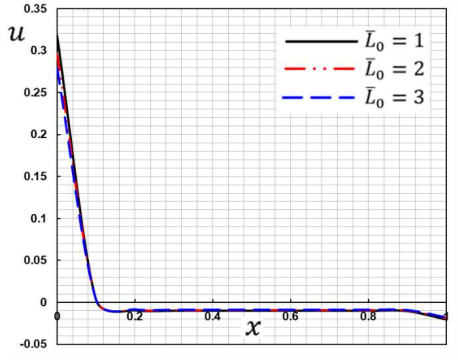

(c) Displacement u versus x.

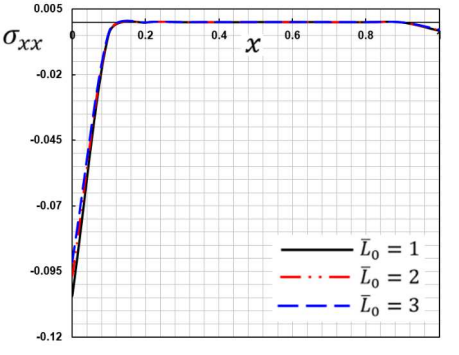

(d) Thermal stress σ_{xx} versus x.

FIG. 5. The transverse deflection, temperature, displacement, and thermal stress distributions of the microbeam for different values of the laser intencity parameter I_0.

When a laser with a short pulse irradiates the surface of the microbeam, the temperature rise speed becomes very fast due to the high energy intensity in a very short time, which causes the temperature gradient to increase significantly. As a result, the deflection w increases rapidly with the laser intensity parameter I_0 and the peak deflection takes place. Over time, the temperature rises rapidly and the temperature gradient decrease, thus deflection weakens to a relatively small value. It is to be noted from these figures that the amplitude of thermal deformation decreases when the heat transfer outside the thermal diffusion zone is reduced.

7.5. The effects of the longitudinal magnetic field on the field quantities

Figure 6 (Case 5) show the variations of the non-dimensional temperature, stress, and displacement, respectively, which demonstrate the effects of the longitudinal magnetic field parameter on the variations of the considered variables.

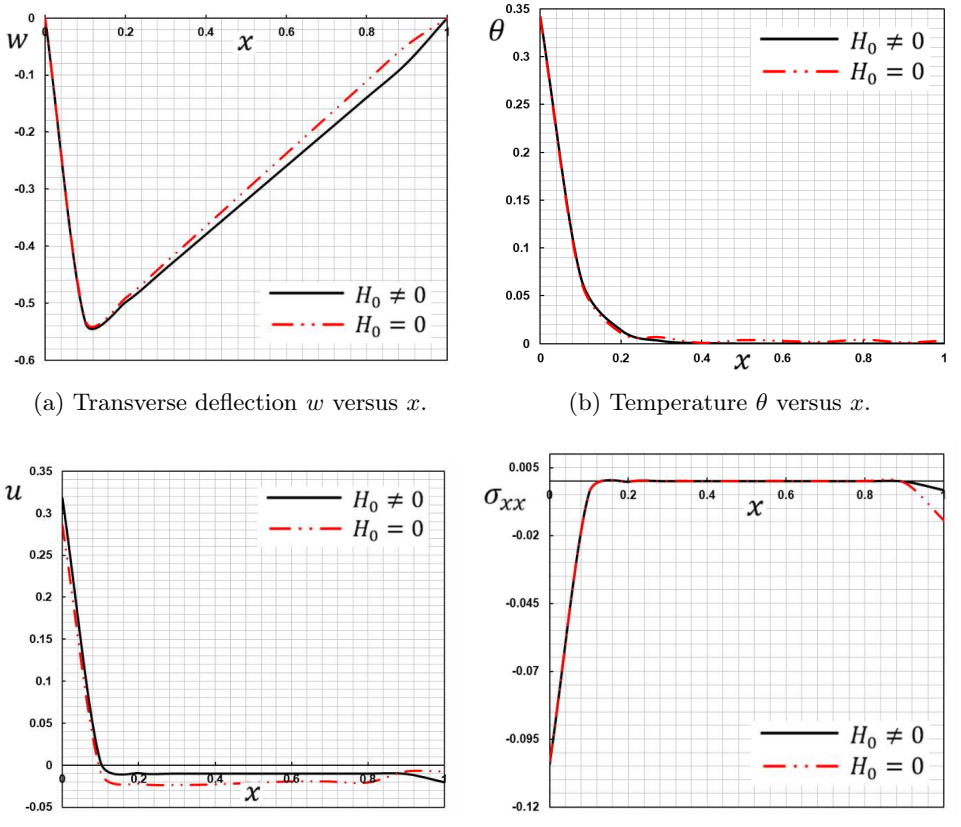

(a) Transverse deflection w versus x.

(b) Temperature θ versus x.

(c) Displacement u versus x.

(d) Thermal stress σ_{xx} versus x.

Fig. 6. The transverse deflection, temperature, displacement, and thermal stress distributions of the microbeam for different values of the longitudinal magnetic field H_0.

If the magnetic field effect is neglected, then the results are in agreement with [46] with suitable modification in the procedure of the solution.

Therefore, the magnetic field has an important influence on the thermal vibration of the resonators of the microresonators. Thus, when designing microresonators, with a high-quality factor and lower energy consumption, consideration must be given to the effect of the permanent magnetic field on the thermal vibration. In addition, our studies reveal that by increasing the intensity of the axial magnetic field, the vibration of the microbeam decreases due to the influence of Lorentz's force and Maxwell stresses the vibrations of small beams. It is worth noting that the impacts of the magnetic field on the thermo-dynamic behavior of the micro-beams were examined in detail [35, 46].

7.6. The effect of the phase lags τ_q and τ_θ on the field quantities

In this case, we consider various values of phase delays of the heat flow and the temperature gradient τ_q and τ_θ, respectively. The graphs in Fig. 7 represent the

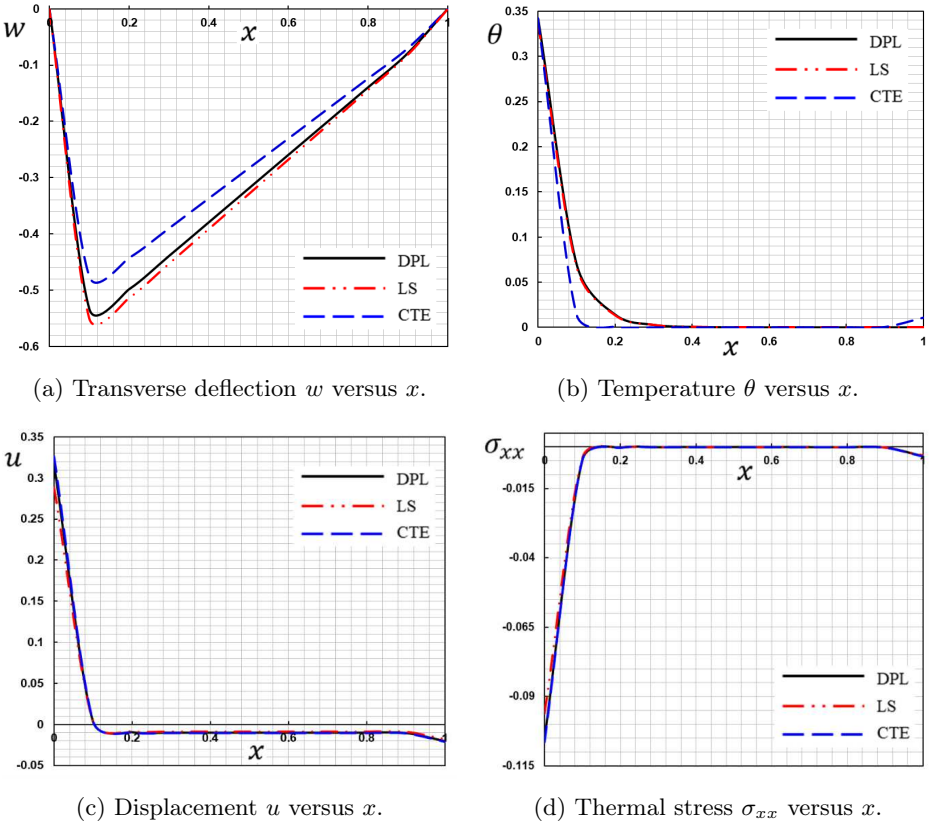

(a) Transverse deflection w versus x.

(b) Temperature θ versus x.

(c) Displacement u versus x.

(d) Thermal stress σ_{xx} versus x.

FIG. 7. The transverse deflection, temperature, displacement, and thermal stress distributions of the microbeam for different values of phase lag parameters τ_1 and τ_θ.

curves that predicted three different thermoelasticity theories obtained as special cases of the DPL model. The computations for different values of the parameters τ_q and τ_θ were performed to get the associated theories: coupled theory (CTE) when ($\tau_q = \tau_\theta$), Lord–Shulman theory (LS) when ($\tau_\theta = 0$, $\tau_q = 0.2$) and finally the Tzou model (DPL) when ($\tau_\theta = 0.1$, $\tau_q = 0.2$).

The classical Fourier model, which leads to an endless propagation speed of thermal energy, is no longer valid in these cases, as many researchers have pointed out. The non-Fourier effect of heat conduction takes into account the effect of mean free time (phase delays) in the energy carrier's collision process, which can eliminate this contradiction.

From the different figures, it is detected that the phase delay parameters have significant implications for the distribution of field quantities. Also, we can note that near the ends of the beam where the boundary conditions predominate, the coupled and the generalized models give results very close. Inside the beam, the solution differs significantly. This is due to the phenomenon that heatwaves in the conventional theory are transmitted with the infinite speed of heat propagation in contrast with the limited speed in the generalized state. Finally, by increasing the distance, the results are very close to one another, which is consistent with the generalized theories of thermal heat.

8. Conclusions

The present study has investigated the thermoelastic vibration of thermo-viscoelastic microbeams at the same time exposed to an axial magnetic force. The upper surface of the microbeam is also excited regularly by a laser pulse and subjected to a thermal load. Using the thermoelastic model with phase-lags, the effects of mechanical relaxations (viscosity), magnetic, the pulse width of varying temperature, and laser pulse parameters on vibrations of nanobeam with clamped-clamped boundary conditions have been evaluated analytically. According to our work, we reached the following conclusion:

- The pulse width of varying temperature plays a significant role in all the field variables. As a short-pulsed laser irradiates the beam's surface, the temperature rise is quick due to a high energy strength in a very short time, which significantly raises the temperature gradient. This results in increasingly rising deflection and peak deflection. Over time, the temperature increases and the temperature drops to a relative lower deflect.
- The laser-pulse and the laser intensity parameters have significant effects on all the studied quantities. Thus, thermodynamics can be seen as a short-term and thin-scale operation. It affects every aspect very quickly, and is therefore harmful,

- The effects of the longitudinal magnetic field on the variations of the considered variables is very clear. Therefore, the magnetic field has an important influence on the thermal vibration of the resonators of the microresonators and should be considered.
- The existence of viscosity terms in the thermoelastic model with phase lags causes significant changes in all the studied fields It must be noted that the magnitude of thermoelastic fields has decreased considerably for viscous cases compared to non-viscous cases.
- It is appropriate to remember that after the peak deflection, the beam reaches a quasi-steady vibration, showing a distinct non-Fourier effect.
- Finally, from the previous analysis it can be concluded that the viscoelasticity and magnetic field effect of materials are gradually applied to the design of the micro-electromechanical systems.

References

1. F.O. OLSEN, L. ALTING, *Cutting front formation in laser cutting CIRP annal*s, Manufacturing Technology, **38**, 1, 215–218, 1989.
2. P. SCHAAF, *Laser nitriding of metals*, Progress in Materials Science, **47**, 1–161, 2002.
3. A.K. DUBEY, V. YADAVA, *Laser beam machining-a review*, International Journal of Machine Tools and Manufacture, **48**, 6, 609–628, 2008.
4. M.I. OTHMAN, A.E. ABOUELREGAL, *The effect of pulsed laser radiation on a thermoviscoelastic semi-infinite solid under two-temperature theory*, Archives of Thermodynamics, **38**, 3, 77–99, 2017.
5. D.W. TANG, N. ARAKI, *The wave characteristics of thermal conduction in metallic films irradiated by ultra-short laser pulses*, Journal of Physics D: Applied Physics, **29**, 2527–2533, 1996.
6. D.Y. TZOU, *Macro- to Micro-Scale Heat Transfer: The Lagging Behavior*, Taylor & Francis, Bristol, 1997.
7. D. JOSEPH, L. PREZIOSI, *Heat waves*, Reviews of Modern Physics, **61**, 1, 41–73, 1989.
8. M.N. OZISIK, D.Y. TZOU, *On the wave theory in heat-conductio*n, Journal of Heat Transfer ASME, **116**, 3, 526–535, 1994.
9. A.M. ZENKOUR, A.E. ABOUELREGAL, *The effect of two temperatures on a functionally graded nanobeam induced by a sinusoidal pulse heating*, Structural Engineering and Mechanics, **51**, 199–214, 2014.
10. A.M. ZENKOUR, A.E. ABOUELREGAL, *Effect of harmonically varying heat on FG nanobeams in the context of a nonlocal two-temperature thermoelasticity theory*, European Journal of Computational Mechanics, **23**, 1–14, 2014.
11. A.M. ZENKOUR, A.E. ABOUELREGAL, K.A. ALNEFAIE, N.H. ABU-HAMDEH, E.A. AIFANTIS, *Refined nonlocal thermoelasticity theory for the vibration of nanobeams induced by ramp-type heating*, Applied Mathematics and Computation, **248**, 169–183, 2014.

12. A.M. Zenkour, A.E. Abouelregal, *Vibration of FG nanobeams induced by sinusoidal pulse heating via a nonlocal thermoelastic model*, Acta Mechanica, **225**, 12, 3409–3421, 2014.

13. A.M. Zenkour, A.E. Abouelregal, *Nonlocal thermoelastic nanobeam subjected to a sinusoidal pulse heating and temperature-dependent physical properties*, Microsystem Technologies, **21**, 8, 1767–1776, 2015.

14. D. Royer, *Mixed matrix formulation for the analysis of laser-generated acoustic waves by a thermoelastic line source*, Ultrasonics, **39**, 345–354, 2001.

15. X. Wang, X. Xu, *Thermoelastic wave induced by pulsed laser heating*, Applied Physics A, **73**, 107–114, 2001.

16. A.M. Zenkour, *Refined two-temperature multi-phase-lags theory for thermomechanical response of microbeams using the modified couple stress analysis*, Acta Mechanica, **229**, 9, 3671–3692, 2018.

17. M.N.M. Allam, A.E. Abouelregal, *The thermoelastic waves induced by pulsed laser and varying heat of inhomogeneous microscale beam resonators*, Journal of Thermal Stresses, **37**, 4, 455–470, 2014.

18. A.K. Soh, Y. Sun, F. Daining, *Vibration of microscale beam induced by laser pulse*, Journal of Sound and Vibration, **311**, 1–2, 243–253, 2008.

19. Y. Sun, F. Daining, M. Saka, A.K. Soh, *Laser-induced vibrations of micro-beams under different boundary conditions*, International Journal of Solids and Structures, **45**, 7–8, 1993–2013, 2008.

20. R. Kumar, *Response of thermoelastic beam due to thermal source in modified couple stress theory*, Computational Methods in Science and Technology, **22**, 2, 87–93, 2016.

21. R. Kumar, S. Devi, *Eigenvalue approach to nanobeam in modified couple stress thermoelastic with three-phase-lag model induced by ramp type heating*, Journal of Theoretical and Applied Mechanics, **55**, 3, 1067–1079, 2017.

22. A. Sur, S. Mondal, M. Kanoria, *Memory response in the vibration of a micro-scale beam due to time-dependent thermal loading*, Mechanics Based Design of Structures and Machines, doi: 10.1080/15397734.2020.1745078, 2020.

23. A. Sur, *Wave propagation analysis of porous asphalts on account of memory responses*, Mechanics Based Design of Structures and Machines, doi: 10.1080/15397734.2020.1712553, 2020.

24. S. Mondal, M. Kanoria, *Thermoelastic solutions for thermal distributions moving over thin slim rod under memory-dependent three-phase lag magneto-thermoelasticity*, Mechanics Based Design of Structures and Machines, **48**, 3, 277–298, 2020.

25. A. Sur, M. Kanoria, *Field equations and corresponding memory responses for a fiber-reinforced functionally graded due to heat source*, Mechanics Based Design of Structures and Machines, doi: 10.1080/15397734.2019.1693897, 2019.

26. S. Mondal, A. Sur, M. Kanoria, *Transient heating within skin tissue due to time-dependent thermal therapy in the context of memory dependent heat transport law*, Mechanics Based Design of Structures and Machines, doi: 10.1080/15397734.2019.1686992, 2019.

27. A.E. Abouelregal, M.A. Elhagary, A. Soleiman, K.M. Khalil, *Generalized thermoelastic-diffusion model with higher-order fractional time-derivatives and four-phase-lags*, Mechanics Based Design of Structures and Machines, doi: 10.1080/15397734 .2020.1730189, 2020.

28. A.C. ERINGEN, *Nonlocal polar elastic continua*, International Journal of Engineering Science, **10**, 1–16, 1972.
29. M.E. GURTIN, J. WEISSMÜLLER, F. LARCHÉ, *A general theory of curved deformable interfaces in solids at equilibrium*, Philosophical Magazine, **78**, 5, 1093–1109, 1998.
30. E.C. AIFANTIS, *Strain gradient interpretation of size effect*s, International Journal of Fracture, **95**, 1–4, 299–314, 1999.
31. A.C. ERINGEN, *Theory of micropolar plates*, Journal of Applied Mathematics and Physics, **18**, 1, 12–30, 1967.
32. R.A. TOUPIN, *Elastic materials with couple-stresses*, Archive for Rational Mechanics and Analysis, **11**, 385–414, 1962.
33. R.D. MINDLIN, H.F. TIERSTEN, *Effects of couple-stresses in linear elasticity*, Archive for Rational Mechanics and Analysis, **11**, 1, 415–448, 1962.
34. A. ZAKRIA A. E. ABOUELREGAL, *Thermoelastic response of microbeams under a magnetic field rested on two-parameter viscoelastic foundation*, Journal of Computational Applied Mechanics, **51**, 2, 332–339, 2020.
35. J. CHEN, E. PAN, H. CHEN, *Wave propagation in magneto-electro-elastic multilayered plates*, International Journal of Solids and Structures, **44**, 1073–1085, 2007.
36. Y. HONG, L. WANG, *Stability and nonplanar buckling analysis of a current-carrying mircowire in three-dimensional magnetic field*, Microsystem Technologies, **25**, 4053–4066, 2019.
37. I.M. WARD, J. SWEENEY, *The mechanical properties of polymers: general considerations*, [in:] Mechanical Properties of Solid Polymers, 2nd ed., Wiley, Hoboken, NJ, USA, 2013.
38. K.C. CHANG, T.T. SOONG, S.-T. OH, M.L. LAI, *Effect of Ambient temperature on viscoelastically damped structure*, Journal of Structural Engineering, **118**, 7, 1955–1973, 1992.
39. M.K. HABIBI, L.H. TAM, D. LAU, L. YANG, *Viscoelastic damping behavior of structural bamboo material and its microstructural origins*, Mechanic of Materials, **97**, 184–198, 2016.
40. H.H. HILTON, S.B. DONG, *An Analogy for Anisotropic, Nonhomogeneous, Linear Viscoelasticity Including Thermal Stresses*, Development in Mechanics, Pergamon Press, New York, 1964.
41. M.H. GHAYESH, *Viscoelastic dynamics of axially FG microbeams*, International Journal of Engineering Science, **135**, 75–85, 2019.
42. A.E. ABOUELREGAL, *Thermoelastic fractional derivative model for exciting viscoelastic microbeam resting on Winkler foundation*, Journal of Vibration and Control, doi: 10.1177/1077546320956528, 2020.
43. M.H. GHAYESH, *Dynamics of functionally graded viscoelastic microbeams*, International Journal of Engineering Science, **124**, 115–131; doi: 10.1016/j.ijengsci.2017.11.004, 2018.
44. A.E. ABOUELREGAL, H. AHMAD, *Thermodynamic modeling of viscoelastic thin rotating microbeam based on non-Fourier heat conduction*, Applied Mathematical Modelling, **91**, 973–988, 2021.
45. B.A. BOLEY, *Approximate analyses of thermally induced vibrations of beams and plates*, Journal of Applied Mechanics, **39**, 212–216, 1972.
46. J.C. MISHRA, S.C. SAMANTA, A.K. CHAKRABARTY, *Magneto-thermo-mechanical interaction in an aeolotropic viscoelastic cylinder permeated by magnetic field subjected to a periodic loading*, International Journal of Engineering Science, **29**, 1209–1216, 1991.

47. S. Mukhopadhyay, *Effects of thermal relaxations on thermoviscoelastic interactions in an unbounded body with a spherical cavity subjected to a periodic loading on the boundary*, Journal of Thermal Stresses, **23**, 675–684, 2000.

48. D.Y. Tzou, *A unified approach for heat conduction from macro-to micro-scales*, Journal of Heat Transfer, **117**, 8–16, 1995.

49. D.Y. Tzou, *Macro- to Microscale Heat Transfer: the Lagging Behavior, Series in Chemical and Mechanical Engineering*, Taylor & Francis: Washington, DC, USA, 1997.

50. A.M. Zenkour, E.O. Alzahrani, A.E. Abouelregal, *Generalized magneto-thermoviscoelasticity in a perfectly conducting thermodiffusive medium with a spherical cavity*, Journal of Earth System Science, **124**, 8, 1709–1719, 2015.

51. A.M. Zenkour, *Thermal-shock problem for a hollow cylinder via a multi-dual-phase-lag theory*, Journal of Thermal Stresses, **43**, 6, 687–706, 2020.

52. A.M. Zenkour, *Exact coupled solution for photothermal semiconducting beams using a refined multi-phase-lag theory*, Optics & Laser Technology, **128**, 106233, 2020.

53. A.M. Zenkour, *Magneto-thermal shock for a fiber-reinforced anisotropic half-space studied with a refined multi-dual-phase-lag model*, Journal of Physics and Chemistry of Solids, **137**, 109213, 2020.

54. A.M. Zenkour, *Refined multi-phase-lags theory for photothermal waves of a gravitated semiconducting half-space*, Composite Structures, **212**, 346–364, 2019.

55. A.M. Zenkour, *Refined microtemperatures multi-phase-lags theory for plane wave propagation in thermoelastic medium*, Results in Physics, **11**, 929–937, 2018.

56. A.M. Zenkour, D.S. Mashat, *A laser pulse impactful on a half-space using the modified TPL–N models*, Scientific Reports, **10**, 4417, 1–12, 2020.

57. H.W. Lord, Y. Shulman, *A generalized dynamical theory of thermoelasticity*, Journal of the Mechanics and Physics of Solids, **15**, 5, 299–309, 1967.

58. X. Wang, X. Xu, *Thermoelastic wave in metal induced by ultrafast laser pulses*, Journal of Thermal Stresses, **25**, 457–473, 2002.

59. M.N. Allam, A.E. Abouelregal, *The thermoelastic waves induced by pulsed laser and varying heat of non-homogeneous microscale beam resonators*, Journal of Thermal Stresses, **37**, 4, 455–470, 2014.

60. A.E. Green, P.M. Naghdi, *Thermoelasticity without energy dissipation*, Journal of Elasticity, **31**, 189–208, 1993.

61. G. Honig, U. Hirdes, *A method for the numerical inversion of the Laplace transform*, Journal of Mathematical Analysis and Applications, **10**, 113–132, 1984.

62. D.S. Mashat, A.M. Zenkour, A.E. Abouelregal, *Thermoviscoelastic vibrations of a micro-scale beam subjected to sinusoidal pulse heating*, International Journal of Acoustics & Vibration, **22**, 2, 260–269, 2017.

Received June 18, 2020; revised version December 25, 2020.
Published online February 22, 2021.